Self-mixing interferometry based on nanometer fringes and polarization flipping

Zhaoli Zeng (曾召利)*, Shulian Zhang (张书练), Shoushen Zhu (朱守深), Wenxue Chen (陈文学), and Yan Li (李 岩)

State Key Lab of Precision Measurement Technology and Instrument, Department of Precision Instruments, Tsinghua University, Beijing 100084, China

**Corresponding author: zsl-dpi@mail.tsinghua.edu.cn*

Received May 11, 2012; accepted July 10, 2012; posted online November 30, 2012

Self-mixing interferometry (SMI) based on nanometer fringes and polarization flipping is realized. The interferometer comprises a single-mode He-Ne laser and a high-amplitude reflectivity feedback mirror. The nanometer fringes are obtained by tilting the external feedback mirror. The fringe density is 35 times higher than that derived with conventional two-beam interference, and each fringe corresponds to a $\lambda/70$ displacement in external cavity length. Moreover, polarization flipping occurs when the external feedback mirror moves in the opposite direction. Such movement can be used to easily distinguish displacement direction. Experimental results show an optical resolution of displacement measurement of 9.04 nm with a range of 100 μm. The proposed SMI presents promising application prospects in precisely measuring displacement and calibrating other micro-displacement sensors because of its optical wavelength traceability.

OCIS codes: 140.1340, 260.1440, 260.3160.

doi: 10.3788/COL201210.121404.

Self-mixing interferometry (SMI) has attracted significant research attention[1−3]. SMI based on the self-mixing effect of lasers can be realized by using an external reflector to couple laser output back into the laser cavity of a self-mixing interferometer. A SMI is similar to a conventional interferometer in that a fringe corresponds to a $\lambda/2$ change in external cavity length. For lasers with a 632.8-nm wavelength, the fringe resolution is 316.4 nm, a value that does not satisfy the requirements of precise displacement measurement. To obtain high resolution, researchers have attempted to directly increase fringe density by optical subdivision[4−8]. Liu *et al.*[5] obtained an optical subdivision factor of 1/2 in their sensors with a $\lambda/4$ plate in the external cavity. Cheng *et al.*[6] achieved an optical subdivision factor of 1/8, but realizing this value entailed constructing a dual-frequency interferometer with numerous optical components. The above-mentioned optical subdivision methods improve resolution only to a limited extent. Another useful electronic subdivision method for improving SMI resolution[9−12] involves using electrical techniques to subdivide the intensities or phases of SMI fringes into a number of subdivisions (e.g., 4, 32, and 64). Electronic subdivision achieves high resolution, but the signal processing circuit is complicated and the SMI signal is prone to interference from electromagnetic environments. Fei *et al.* reported a novel method[13] that yields high optical resolution because of nanometer fringes. This method easily distinguishes displacement direction through polarized flipping, which depends on the motion of the external cavity. This technique also features simple optical configuration and signal processing. Moreover, it can be used to calibrate other micro-displacement sensors because of its optical wavelength traceability.

In this letter, we realize integrated SMI based on nanometer fringes and polarization flipping. The interferometer is made up of an optical source, an external reflector, and a signal processing circuit. Theoretical analysis and test results are presented. The contrast results of the proposed SMI and the PI nanopositioning system show that the resolution of displacement measurement is 9.04 nm. The error source of the instrument is also discussed.

The system configuration of the SMI is shown in Fig. 1. External feedback mirror 2 is fixed on PI linear stage 1 (P-621.1CD), which has a range of approximately 110 μm. The 632.8-nm He-Ne laser is composed of plane mirror, concave mirror, and laser capillary. Wollaston prism is used to separate the two polarized modes, which are detected by photoelectric detectors (D_1 and D_2). The single-mode laser and photoelectric detection elements are packaged by instrument shell to enable the construction of the optical gauge head. Signal processing circuit is integrated in an electrical cabinet located far from the gauge head.

At a strong feedback level, the multiple feedback effects should be considered; the complex effective field amplitude reflectivity caused by the laser coupling mirror and external feedback mirror can be expressed as

$$r_{\mathrm{eff}} = r_2 - (1 - r_2^2) r_3 \sum_{n=1}^{m} (r_2 r_3)^{n-1} f_n \exp(\mathrm{i} n \omega \tau_1), \quad (1)$$

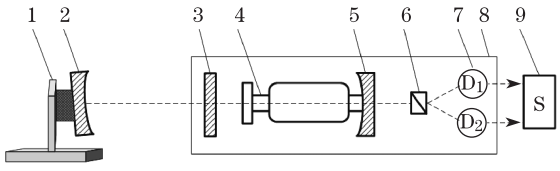

Fig. 1. Schematic of erperimental setup. 1: PI linear stage; 2: external feedback mirror; 3: laser cavity mirror; 4: laser capillary; 5: laser cavity mirror; 6: Wollaston prism; 7: photoelectric detectors (D_1,D_2); 8: instrument shell; 9: signal processing circuits.

where r_2 and r_3 are the amplitude reflection coefficients of the mirrors, n represents the beam's nth round trip in the external cavity (also called the feedback order), ω denotes the optical angular frequencies, τ_1 represents the round-trip time of the laser beam in the external cavity, and f_n is the coupling efficiency of the nth-order feedback beam.

As indicated in Eq. (1), the multiple high-order feedback beams reenter the laser cavity because of the strong feedback, which results in high-density fringes. Fringe density is determined by feedback order. The coupling efficiency of the nth-order feedback beam is determined by the tilt angle of the feedback mirror when the laser is selected. When θ increases, the relative increment in the coupling efficiency of the higher order feedback beams is larger than that of the lower order feedback beams. After this increase, the fringe intensities tend to be uniform.

The nanometer fringes are obtained when $\theta = 1.5$ (Fig. 2(b)). The fringe density is dozens of times higher than that derived by conventional feedback (Fig. 2(a)). In particular, the laser polarization state flips when the motion direction of the feedback mirror changes. This result can be used to distinguish displacement direction.

The electronic circuit for signal processing is simple, as shown in Fig. 3(a). The amplified intensity signals are sent to comparators, which reshape the signals to square ones. The square pulses are shown in Fig. 3(b). When the PZT voltage is low, i.e., the feedback mirror moves close to the laser, the square pulse of the $P_{//}$ light is generated and the $P_{\perp}$ light is in a high logic state. When the PZT voltage is high, i.e., the feedback mirror moves away from the laser, the square pulse of the $P_{\perp}$ light is generated and the $P_{//}$ light is in a high logic state. The square pulse is then sent to a counter to determine the number of fringes by which the displacement of the feedback mirror is obtained. The displacement direction is also easily determined by the square pulses of $P_{//}$ and $P_{\perp}$, which have different states when the feedback mirror moves in the opposite direction.

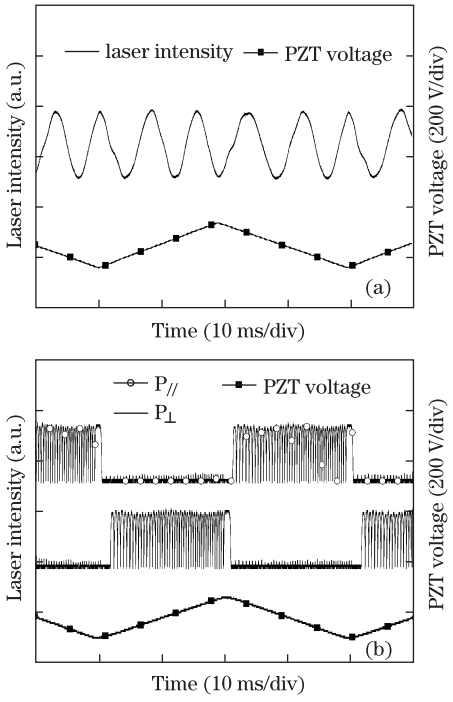

Fig. 2. Self-mixing interference fringes at different feedback levels. (a) Intensity fringes of conventional weak feedback; (b) nanometer fringes and polarization flipping in self-mixing interference at strong feedback levels.

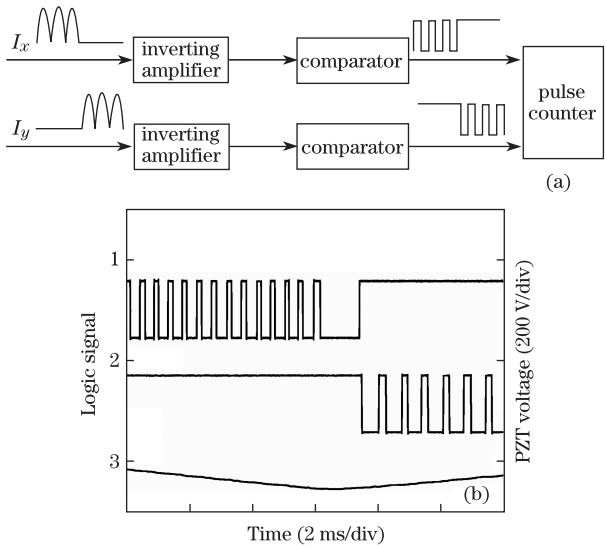

Fig. 3. Flowchart of the signal processing for the displacement sensor. Trace 1: the square pulse of the $P_{//}$ light; Trace 2: the square pulse of the $P_{\perp}$ light; Trace 3: the driven voltage of PZT.

The SMI resolution is tested by measuring the displacement of the PI nanopositioning system, which has a resolution of 0.4 nm and a repeatability of 2 nm. The feedback mirror is fixed onto the PI stage, and the external cavity length is about 60 mm. When the nanometer fringes are obtained, the angle of the feedback mirror becomes invariable during measurement. The PI stage is driven by closed-loop controller (E-753.1CD) from 0 to 100 μm. The pulse numbers that are generated by the 100-μm displacement of M_3 and the results are displayed on the liquid crystal display (LCD) of the electrical cabinet. The average pulse numbers of 0–100 μm is 11062, which is regarded as the measurement result in the range of 100 μm. Thus, pulse equivalent δ is approximately 100/11062 μm. Maximal feedback order n can be calculated as $\lambda/2\delta = 35$ because feedback order n should be an integer. This calculation indicates that the fringe density is 35 times higher than that derived under conventional feedback and that the accurate resolution of the self-mixing laser feedback interferometer is $\lambda/70$ (approximately 9.04 nm).

The calibration process is similar to the experiment described above. The contrast results of the SMI and PI nanopositioning system are determined by synchronously measuring the displacement with a step of 10 μm (Fig. 4). The proposed SMI exhibits good stability, and linearity is about 5×10^{-5}.

In addition, the displacement measurement is verified for the triangular vibration of the target. The target is driven by the PI stage with a displacement of 10 μm and a frequency of 2 Hz. The measurement result is shown in Fig. 5, which indicates that the maximal measurement error does not exceed 10 nm.

The experimental results confirm the feasibility of SMI based on nanometer fringes and polarization

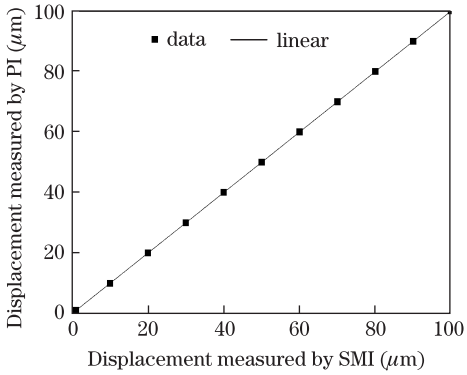

Fig. 4. Contrast results of the proposed SMI and PI nanopositioning system.

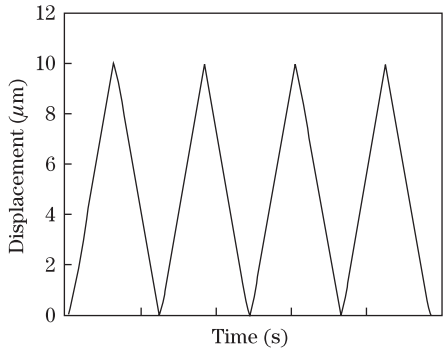

Fig. 5. Displacement measurement result for the target.

flipping. This approach exhibits a high optical resolution of 9.04 nm in a 100-μm range. In practice, however, the accuracy of displacement measurement is influenced by many factors.

Firstly, the accurate wavelength value is unknown because the laser is not frequency stabilized. When $L = 170$ mm, the longitudinal mode interval is almost 880 MHz, and the frequency drift is less than ± 440 MHz from the central frequency for it to remain a single-mode output. Under typical room conditions, therefore, the maximum wavelength error induced by the frequency drift is

$$\Delta\lambda_{\max} = \frac{\lambda_0^2}{c}\Delta\nu_{\max}, \quad (2)$$

where λ_0 is the wavelength in vacuum, and c is the light velocity in vacuum. The relative error of wavelength $\Delta\lambda_{\max}/\lambda$ does not exceed 0.92×10^{-6}. For the 1-mm range, the measurement error is $\Delta_1 = 0.92 \times 10^{-6} \times 1$ mm=0.92 nm.

Secondly, after measurement, SMI may not produce a complete fringe and result in errors if displacement is smaller than resolution ($\lambda/70$). When the intensity of the last fringe is smaller than the threshold value, the comparator does not generate a count pulse, and the measurement result is lower than the actual value. When the intensity of the last fringe is greater than the threshold value, the comparator generates a count pulse, and the measurement result is greater than the actual value. However, maximum errors of this kind do not reach more than one count pulse, which is $\Delta_2 = \lambda/70 = 9.04$ nm.

Thirdly, under typical room conditions without the constant temperature method, temperature changes can induce variations in the air refractive index. The variations in air refractive index (Δn) can be estimated using the Ellen formula:

$$\Delta n = (0.00268\Delta p - 0.929\Delta t - 0.00042\Delta f) \times 10^{-6}, \quad (3)$$

where Δp, Δt, and Δf are the variations in air pressure, temperature, and humidity, respectively. In an experimental environment, the variations in air pressure and humidity can be disregarded. The variation in temperature is about 1 °C. Consequently, the variation in Δn is less than 0.93×10^{-6}. Thus, this part of the error is $\Delta_3 = 0.93 \times 10^{-6} \times 1$ mm=0.93 nm.

Finally, combined estimation error Δ is

$$\Delta = \sqrt{\sum_{i=1}^{3} \Delta_i^2} = 9.1 \text{ nm}. \quad (4)$$

In conclusion, SMI based on nanometer fringes and polarization flipping is realized. The method exhibits high optical resolution without the need for electronic subdivision technology. Furthermore, the displacement direction can be easily determined by polarization flipping. The SMI resolution is 9.04 nm and the combined estimation error is 9.1 nm. This SMI approach presents good potential application prospects in precise displacement measurement. It is particularly advantageous in the calibration of other micro-displacement sensors because of its optical wavelength traceability.

This work was supported by the Key Project of the National Natural Science Foundation of China (Nos. 60827006 and 60723004) and the Scientific and Technological Achievements Transformation and Industrialization Project by the Beijing Municipal Education Commission.

References

1. D. E. T. F. Ashby and D. F. Jephcott, Appl. Phys. Lett. **3,** 13 (1963).
2. R. C. Addy, A. W. Palmer, and K. T. V. Grattan, J. Lightwave Technol. **14,** 2676 (1996).
3. Y. D. Tan and S. L. Zhang, Appl. Opt. **46,** 6064 (2007).
4. Z. Zhao and S. Zhang, Chin. Opt. Lett. **10,** 032801 (2012).
5. G. Liu, S. L. Zhang, and J. Zhu, Appl. Opt. **42,** 6636 (2003).
6. Z. Cheng, H. Gao, Z. Zhang, H. Huang, and J. Zhu, Appl. Opt. **45,** 2246 (2006).
7. W. Mao, S. Zhang, and L. Fei, Appl. Opt. **45,** 8500 (2006).
8. X. Cheng, S. Zhang, L. Zhang, and Y. Tan, Chin. Phys. Lett. **23,** 3275 (2006).
9. B. Ovryn and J. H. Andrews, Opt. Lett. **23,** 1078 (1998).
10. J. Kato, N. Kikuchi, I. Yamaguchi, and S. Ozono, Meas. Sci. Technol. **6,** 45 (1995).
11. T. Suzuki, S. Hirabayashi, O. Sasaki, and T. Maruyama, Opt. Eng. **38,** 543 (1999).
12. M. Wang and G. Lai, Rev. Sci. Instrum. **72,** 3440 (2001).
13. L. Fei and S. Zhang, Opt. Commun. **273,** 226 (2007).